RSC Advances

PAPER

View Article Online
View Journal | View Issue

CrossMark click for updates

Cite this: *RSC Adv.*, 2016, **6**, 12422

Nisin anchored cellulose nanofibers for long term antimicrobial active food packaging

Seema Saini,[ab] Cecile Sillard,[ab] Mohamed Naceur Belgacem[ab] and Julien Bras*[ab]

Received 29th October 2015
Accepted 8th January 2016

DOI: 10.1039/c5ra22748h

www.rsc.org/advances

Increasing consumer demand for high performance bio-based materials in order to develop microbiologically safer foods has forced the food industry to revise their packaging strategies. One of the emerging fields within this industry is active packaging which prevents an excess of antimicrobials in food formulation and, meanwhile, inhibits or reduces bacterial growth. In this study, a green process of immobilizing a peptide on bio-based carboxylated cellulose nanofibers (CNF) using a coupling agent has been proposed. Validity of the grafting reaction between nanocellulose, the coupling agent and peptide was first analyzed by Quartz crystal microbalance-dissipation (QCM-D). Efficiency of the grafting reaction was characterized with Fourier Transform Infrared spectroscopy and thermogravimetric analysis which suggest the grafting of nisin on CNF. Finally, the amount of grafted nisin was quantified on the surface of CNF by conductometric titration and nitrogen content analysis. The antimicrobial activity and release experiment demonstrated that the nisin grafted CNF displayed excellent antimicrobial activity against different Gram +ve bacteria (*Bacillus subtilis* and *Staphylococcus aureus*) with significant 3.5 log reduction. The obtained results are promising and confirm the interest in such strategy.

Published on 13 January 2016. Downloaded on 1/26/2026 10:23:08 AM.

Introduction

Infectious diseases frequently spread through food quality deterioration. According to the World health organization, globally, 351 000 people die every year due to food poisoning.[1] Therefore, to assure the safety of food products, it is necessary to control the contamination by limiting the growth of pathogenic bacteria during processing and storage.

In traditional packaging, antimicrobial active compounds are mixed with the food formulation for preservation. But, the presence of antimicrobials in the bulk is unable to target the food surface where a large portion of spoilage and contamination occurs. Hence, bioactive antimicrobial packaging was introduced as an innovative approach to diminish microbial growth predominantly at the surface of food.[2,3] Various researchers have demonstrated the use of antimicrobial compounds, such as organic acids (sorbic acid, acetic acid), essential oils (thymol, rosemary oil), enzymes (lysozyme), bacteriocins (nisin and pediocin), and metal particles (silver, zinc oxide)[4–7] incorporated or coated over polymer matrices.

Indeed, this study primarily focuses on the use of a cationic, amphiphilic antimicrobial peptide nisin composed of 34 amino acids produced by strains of the bacterium *Lactococcus lactis lactis*.[8] Nisin has already been exploited for decades as a food preservative and is also approved by the European food safety authority with acceptable uptake of 0.13 mg per kg per day per person.[9]

Nisin intervenes with cell wall synthesis by binding to lipid II, a core precursor of cell wall synthesis, and efficiently permeabilizing the cell membrane *via* the formation of pores.[10] Converse to antibiotics, their mode of action does not encourage pathogenic resistance, hence, suppresses the evolution of new infectious diseases.[11]

In last decade, nisin has been either incorporated into various polymer matrices, for instance polyethylene brushes,[12] LDPE,[13] polypropylene,[14] soy protein,[15] or starch,[16] or in coatings over them[17–19]_ENREF_17. However, these direct applications have been limited in their beneficial effects and exhibit a loss in long-term activity.

Still, only very few investigations have taken place with chemical covalent immobilization of nisin for example some studies tried to graft nisin on compounds such as multiwalled carbon nanotubes,[20] or calcium alginates.[21–23]

Due to bio-based material requirements and needs from society, intensive research is being carried out to develop environmentally-friendly packaging materials to replace petroleum-based synthetic polymers. Nevertheless, by virtue of its properties (renewable, biodegradable, biocompatible and cost effective), cellulose carry on gaining attention for bioactive packaging.[24,25]

Cellulose nanofibers (also called microfibrillated cellulose or nanofibrillated cellulose) is a novel cellulosic nanomaterial developed by a researcher team at ITT Rayonier Inc. in 1983.[26] These slender materials possess a diameter between 10–50 nm

[a]*Univ. Grenoble Alpes, LGP2, F-38000 Grenoble, France*
[b]*CNRS, LGP2, F-38000 Grenoble, France. E-mail: Julien.Bras@grenoble-inp.fr*

This journal is © The Royal Society of Chemistry 2016

Published on 13 January 2016. Downloaded on 1/26/2026 10:23:08 AM.

and length >1 μm. CNF is a very promising material with unique properties such as being light-weight, low density, high barrier, low coefficient of thermal expansion, extremely high surface area, flexible, and good strength properties.[27–29] It is prepared by high shearing mechanical disintegration[26] which is major concern in its preparation as fibrillation consume energy as high as 78.8 MJ kg^{-1}.[30]

Pretreatment of the cellulose fibers before mechanical disintegration, not only decreases the energy consumption, but can also add novel surface properties to fibers. Thus, pretreatment with 2,2,6,6-tetramethylpiperidine-1-oxyl (TEMPO) selectively converts the C6 groups of primary hydroxyl into carboxyl functions, which attracts attention for diverse applications.[31,32]

Very recently, conventional CNF have been grafted with silanes, isocyanate, anhydrides, isothiocyanate and antibiotics[33–39] to impart antimicrobial properties. The novelty of this work lies in the selection of the type of CNF and active molecule (nisin), which was never attempted in previous investigations. It also proposes to use a new green strategy for grafting active molecule. Indeed even if such grafting has been recently performed onto nanocellulose for various molecules, none of them targeted antimicrobial properties using rather large molecule weight molecule like nisin.

Consequently, in this study, we have developed a novel antimicrobial film with covalently linked nisin on the surface of TEMPO oxidized CNF especially for food packaging. In addition to reduction of energy consumption during mechanical disintegration of fibers, TEMPO pretreatment imparts additional properties to nanofibers which could be exploited for different application. Our novel TEMPO oxidized CNF film has enhanced the antimicrobial activity of the film against *Bacillus subtilis* and *Staphylococcus aureus*.

Materials and methods

Materials

For the preparation of nanocellullose, high quality bleached softwood cellulose (domsjo, Sweden) produced from a controlled mixture of spruce and pine (respectively 60% and 40%) was used. Nisin Z was procured by Handary S.A. Various chemicals were purchased such as 2,2,6,6-tetramethylpiperidine-1-oxyl radical (Sigma Aldrich), 2-(*N*-morpholino)ethanesulfonic acid (sigma Aldrich), *N*-hydroxysuccinimide (Sigma Aldrich), 1-ethyl-3-(3-dimethylaminopropyl)carbodiimide (Sigma Aldrich), L-α-lecithin (Merck), sodium thiosulphate (Roth), L-histidine (Merck), Tween 80 (Merck), potassium dihydrogen phosphate (KH_2PO_4) (Roth). A suspension of *Bacillus subtilis* (10^7 spores per mL) was also purchased from Humeau (France). Spores were revived by growing in nutrient broth for 16 hours. A nutrient agar adapted to the development of the spores was also purchased from Humeau (France). *Staphylococcus aureus* ATCC 6538 was bought from Thermo scientific, USA. Petri dishes with a diameter of 90 mm and 60 mm were purchased from Roth (France) and used for the antibacterial tests.

Preparation carboxylated CNF

The dried cellulose fibers (15 g) were soaked in water (1 L) overnight aiming for a better dispersion of fibers during reaction. After redispersion, the cellulose fibers were transferred to a reactor with heating mantle, after TEMPO (0.24 g, 0.1 mmol) and sodium bromide (1.5 g, 1 mmol) were added. The TEMPO-mediated oxidation was started by pouring the 4.9 mL of the sodium hypochlorite solution (5.0 mmol NaClO per gram of cellulose at pH 10) slowly into the reactor and then consistency was filled with deionised water till 1.5 L. Then, the reaction was carried out at room temperature by stirring at 200 rpm. The pH was maintained at 10 by adding 0.5 M sodium hydroxide (NaOH) using a pH regulator until no further decrease of pH was observed.

The reaction was quenched by lowering the pH till 7 with 0.1 M HCl. TEMPO-oxidized cellulose was thoroughly washed with deionized water by vacuum filtration using a nylon sieve with a pore diameter of 1 μm until the filtrate conductivity value reached less than 5 μS cm^{-1}. After that, the TEMPO cellulose was stored at 4 °C for further treatment. Recovery ratios of the TEMPO oxidized celluloses after washing were over 90%. The carboxylate content of the TEMPO-oxidized cellulose was determined using conductivity titration method. For the preparation of nanofibers, the pretreated fibers were passed through Masuko® grinder at 2500 rpm for 45 min under continuous recirculation.[40]

Chemical grafting of nisin on carboxylated CNF

1 g of dry TEMPO CNF was diluted with 160 mL 2-(*N*-morpholino)ethanesulfonic acid (MES) buffer (pH 4.5; MES 10 mM). The CNF suspension was stirred for 30 minutes. 0.84 g of EDC (1-ethyl-3-(3-dimethylaminopropyl)carbodiimide) was solubilized in 10 mL of MES buffer; 0.5 g of NHS (*N*-hydroxysuccinimide) was solubilized in 10 mL of MES buffer. The required quantity of nisin was added to the TEMPO CNF suspension and then, EDC–NHS was added to the mixture. Finally the mixture was stirred during 24 hours at room temperature.

The quantity of nisin was calculated on the basis carboxyl group on the surface of CNF. Two quantities were used to analyze the efficiency of grafting *i.e.* 1 and 4 equivalents with respect to the carboxyl group.

Validation of grafting reaction between CNF and nisin (QCM-D)

Adsorption measurements were performed with a Quartz Crystal Microbalance with Dissipation (QCM-D). The instrument (Q-Sense® E1, Biolin Scientific, Sweden) measures the resonance frequency of the oscillation of a quartz crystal based on the fundamental frequency (5 MHz) and selected overtones (15, 25, 35, 45, 55, and 75 MHz). However, only the seventh overtone is used in the data evaluation. Sorption curves were acquired using 100 nm gold-coated quartz crystals (QSX301, Biolin Scientific, Sweden). All measurements were performed under constant flow rate (100 μL min^{-1}) and temperature

Published on 13 January 2016. Downloaded on 1/26/2026 10:23:08 AM.

(23 °C). The adsorbed mass (ng nm^{-2}) was estimated from the frequency change (Δf) using Sauerbrey's equation.[41]

$$\Delta f_m = \frac{-2\ {f_0}^2 \Delta m}{A\ \sqrt{\rho_q \mu_q}} \quad (1)$$

where: Δf_m = change in frequency, f_0 = fundamental frequency, Δm = change in mass, A = piezo-electrically active area, ρ_q = density of quartz (2.648 g cm^{-2}), and μ_q = shear modulus of quartz (2.947×10^{-11} dynes per cm^2).

Grafting characterization

Attenuated total reflectance-Fourier transform infrared spectroscopy (ATR-FTIR). ATR-FTIR spectra were recorded for neat and modified CNF in mode, using a Perkin Elmer Spectrum 65. All spectra were recorded between 4000 and 700 cm^{-1}, with a resolution of 4 cm^{-1} and 16 scans. All spectra were manually corrected for its baseline and then normalized according to the band at 1110 cm^{-1}.

Nitrogen content. Nitrogen contents were measured for unmodified and nisin modified CNF at "Service central d'analyse (Vernaison, France)". For each sample, duplicates were performed and the values were averaged.

Thermogravimetric analyses (TGA). A Perkin Elmer Simultaneous thermal Analyzer (STA 6000) was used. About 30 mg of sample was placed in a pan and tested at a heating rate of 10 °C min^{-1} from ambient temperature to 900 °C, under air. All experiments were performed at least twice.

Atomic force microscopy (AFM). Neat CNF and grafted CNF were imaged using Atomic Force Microscope, AFM, (Nanoscope III, Veeco, Canada) characterized in tapping mode with a silicon cantilever (OTESPA, Bruker, USA) on a diluted suspension. Each sample was characterized in tapping mode with a silicon cantilever (OTESPA, Bruker, USA) at different locations. Images were subjected to the first order polynomial flattening in order to reduce the effects of bowing and tilt.

Conductometric titration. Conductometric titration was carried out to obtain the total carboxyl groups in the neat and grafted CNF film. Typically, 0.2 g of dry CNF film was titrated with 0.01 M NaOH (aq.) by adding approximately 0.1 mL in 30 second intervals. Total carboxylate content was calculated by on the basis of the used NaOH volume as follows:

$$X = \frac{C_{NaOH} \times V_2}{m} \quad (2)$$

with X as the total carboxylate content in the sample, C_{NaOH} the exact concentration of the sodium hydroxide solution in μmol L^{-1}, V_2 the volume of the sodium hydroxide solution consumed in the 2nd intersection point for weak acids, in liters and m the oven dry weight of sample.

Finally, percentage of grafting was determined using the total carboxylate content before and after the reaction on each sample:

$$\text{Grafting efficiency } (\%) = 100 \times \frac{X_{(\text{reference})} - X_{(\text{samples})}}{X_{(\text{reference})}} \quad (3)$$

where, $X_{(\text{reference})}$ is total carboxylate content of the neat CNF and $X_{(\text{sample})}$ is the total carboxylate content of the nisin-grafted CNF.

Antibacterial activity

Qualitative assessment of antimicrobial releasing activity. Qualitative antimicrobial activity was analyzed with AFNOR EN 1104 standard by placing circular film of 20 mm diameter onto pre-inoculated agar (with *B. Subtilis*) then incubated for 3 days at 30 °C. The leaching ability of modified CNF was concluded measuring the diameter of the inhibition zone. All experiments were repeated three times.

Quantitative assessment of antimicrobial activity. The quantitative assessment of the antibacterial activity against *B. subtilis* and *S. aureus* was based on the AATCC Test Method 100 (1998) under static conditions. The cell suspensions were prepared with 20 mL of nutrient broth and were grown overnight at 37 °C under horizontal shaking at 200 rpm. An aliquot of 200 μL of cell suspension was then placed onto at least 2 replicates of each sample (modified and unmodified surfaces). After 24 hours of incubation at 37 °C, the bacteria were extracted by using 50 mL of neutralizing solution: L-α-lecithin 3 g L^{-1}, sodium thiosulphate 5 g L^{-1}, L-histidine 1 g L^{-1}, Tween 80 30 g L^{-1}, and a buffer solution (KH_2PO_4 0.68 g L^{-1}) 10 mL L^{-1}, (pH at 7.2 ± 0.2). The numbers of colony forming units (CFU) within the resulting suspensions are then enumerated using the plate count method. The bacteria log reduction, *i.e.* the antibacterial activity of the films, was calculated according to the following formula:

$$\log \text{reduction} = \log \text{CFU } T_{24} \text{ untreated sample} - \log \text{CFU } T_{24} \text{ treated sample} \quad (4)$$

All experiments were at least duplicated.

Results and discussion

Influence of the coupling agent on the interaction between CNF and nisin

First, tempo oxidised cellulose was prepared and characterized. Gel like suspension and semi-transparent dried film was obtained as expected. Morphological nanostructure was confirmed by the AFM as detailed later in Fig. 5. Dimension of CNF calculated with the image J are 18 ± 4 nm which was in the range of classic Tempo CNF.

Since, this was the first investigation for such strategy, it was extremely important to confirm the efficacy of nisin immobilization on the surface of nanofibers with the coupling agent. Therefore, Quartz Crystal Microbalance with Dissipation Monitoring (QCM-D) was first used to monitor the validity of the grafting reaction. QCM-D is a highly sensitive technique which is used to study the reaction binding kinetics of a molecule by analyzing its sorption and desorption from the quartz surface. Two different deposition cycles were preformed using CNF and nisin.

A detailed description of the QCM-D, which represents the normalized change in frequency and dissipation of the 7th

 This journal is © The Royal Society of Chemistry 2016

Published on 13 January 2016. Downloaded on 1/26/2026 10:23:08 AM.

overtone in each deposition cycle, is shown in Fig. 1. In first experiment, nisin solution (1 g L^{-1}) was directly in the flow contact on the carboxylated nanofibers previously coated on the functionalized gold plates.

The introduction of carboxylated CNF on PEI treated gold quartz results in the decrease of the Δf (−30 Hz) and an increase in the corresponding ΔD. This change is attributed to the strong absorption of cellulose on the PEI. After each deposition, the quartz was rinsed with deionized water to remove the excess of unbound compound and to negotiate the frequency response generated by them.

Next, when peptide was passed into QCM-D module, there is instantaneous decrease in Δf and increase in ΔD in less than 2 minutes corresponding to the strong adsorption of nisin on the nanofibers. After 3 minutes of deposition, there was slow depression which was contributed by swelling of the Tempo CNF owning to the absorption of water. The adsorption of nisin on CNF is mainly related to the weak forces such as hydrogen bonding and van der Waals interactions between the two.

In another system of deposition, EDC/NHS was first absorbed on the surface of CNF and then nisin was allowed to interact with EDC/NHS. The EDC/NHS treatment of oxidized nanofibers film decreased the frequency (change over −44 Hz after rinsing) which indicates the formation of semi-stable NHS-esters. It is worthy to notice that no significant desorption of NHS-ester took place even after washing for 20 minutes. Nonetheless, these systems were found to differ with respect to the absorption of nisin. There is very low change in dissipation energy due to the formation of NHS ester, which reduces the swelling of the TEMPO CNF, thus resulting in a rigid layer of nisin which indeed confirms the reaction of CNF with nisin.[42,43]

The mass/thickness of the layers can be determined by the Sauerbrey equation. However, this equation is only applicable to rigid layers. Another indication of a non-rigid viscoelastic film, which leads to a deviation from the Sauerbrey relation, is the frequency dependence of the overtones ($\Delta f/n$). The mass for the coupled TEMPO CNF after water rinsing was found to be 6 mg m^{-2} which corresponds the thickness of 4 nm on the gold surface considering a cellulose nanofibril density of 1500 kg m^{-3}. The mass of CNF was quite sufficient for uniform distribution on the gold plate reducing the non-specific adsorption of nisin on gold plates.[44]

AFM images are recorded to control the morphology of the cellulose after each injection (Fig. 2). No large voids or pores were observed indicating the uniform distribution of TEMPO oxidized cellulose nanofibrils on the surface of the PEI treated gold surface. When EDC/NHS was deposited on the surface of cellulose, a gel like structure was formed with water and NHS/EDC, however, after rinsing and addition of nisin, fibrillar structure similar to the reference CNF was observed.[45] EDC/NHS removes the charge on the nanofibrils by forming NHS esters that reduce the water binding capacity of fibrils. Therefore, rigid absorption of peptide nisin took place mainly on the CNF film surface, when EDC–NHS coupling agent is used.

Grafting of CNF with nisin

Actually, the pathway for covalent immobilization of nisin peptides on the surface of CNF consists of two prime steps. In a first step, COOH on nanofibers were activated by using an EDC–NHS mixture. Then, the nisin peptide was covalently immobilized onto the surface through the nucleophilic reaction occurring between the terminal NH_2 group of the peptide and the activated carboxylic functional group of the surface. Fig. 3

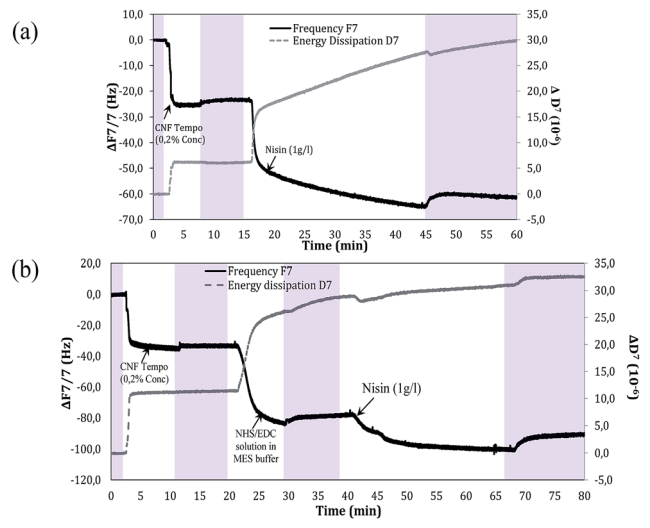

Fig. 1 Frequency and dissipation response of the 7th overtone produced by the absorption on PEI treated gold quartz sensor (a) injection of CNF Tempo (0.2%) and then nisin (1 g L^{-1}) (b) injection of CNF tempo (0.2%) then 2nd injection with EDC/NHS solution in MES buffer, after final injection with nisin (1 g L^{-1}). Pink area represents the washing after each injection with deionized water.

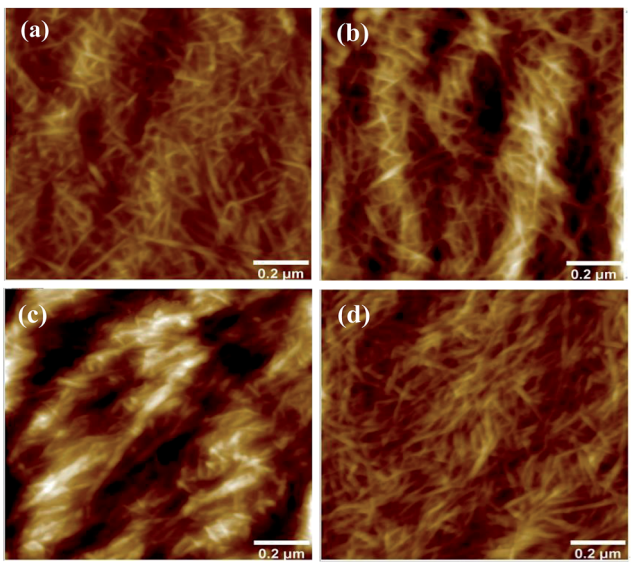

Fig. 2 AFM standard tapping mode height sensor images in air of quartz gold sensors after each deposition cycle (a) nanocellulose (b) nanocellulose–peptide nisin (c) nanocellulose–EDC/NHS (d) nanocellulose–EDC/NHS-nisin. z ranges from −19 to 20.6 nm.

Published on 13 January 2016. Downloaded on 1/26/2026 10:23:08 AM.

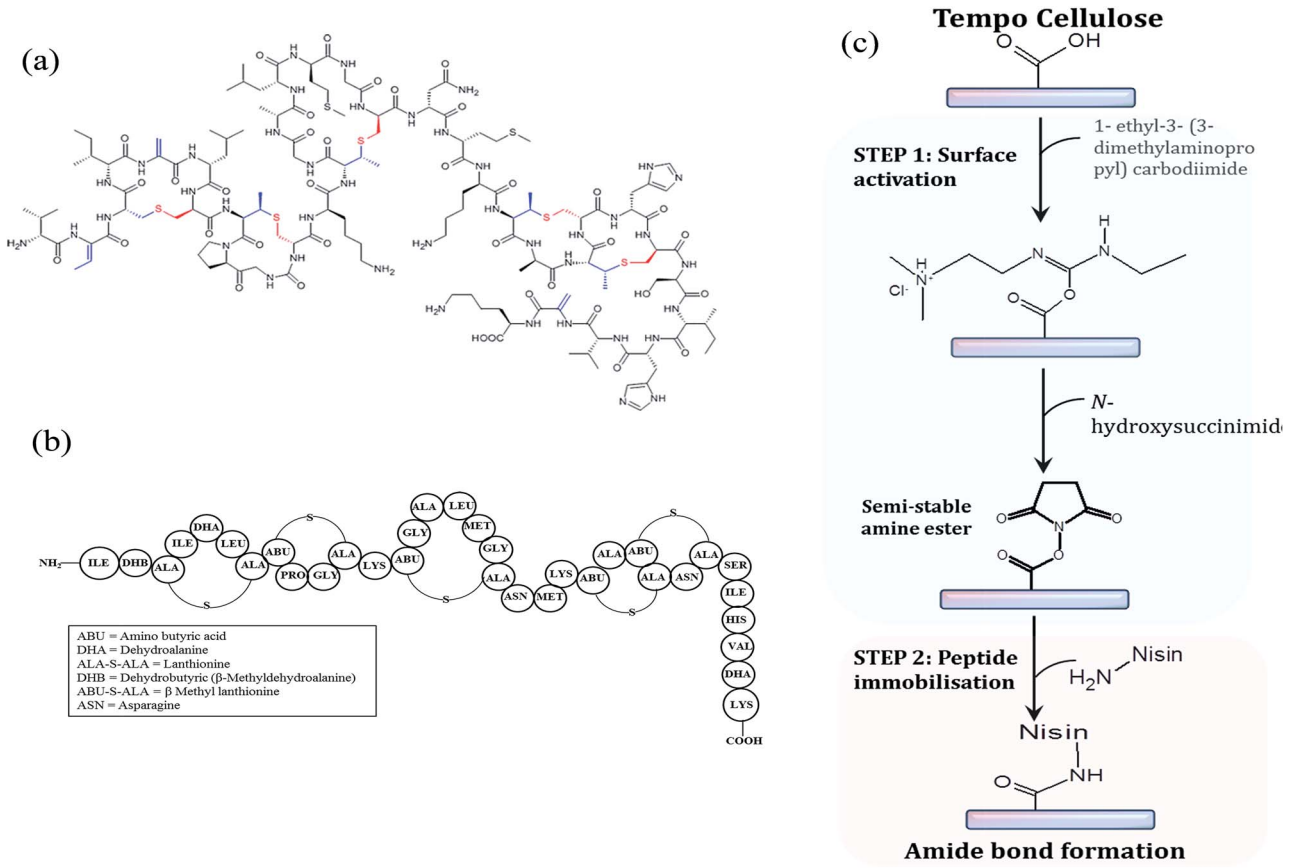

Fig. 3 (a) Chemical structure of the lantibiotic nisin Z (b) primary structure of nisin Z (nisin Z contain asparagine instead of histidine at position 27) (c) schematic illustration of the main steps involved in the grafting of peptide nisin Z on the surface of tempo cellulose.

illustrates the structure of nisin and the reaction pathway demonstrating the main steps involved in the grafting of nisin peptide.

This EDC–NHS intermediate grafting reaction is well known by peptidic reaction but is still barely used with nanocellulose, only very recent papers deals with such strategy and up our knowledge; nobody used it for grafting the peptide on Tempo CNF.[46–49] In this case the risk of "homopolymerisation" (condensation) of nisin is present and can be limited by favoring the adsorption of EDC–NHA as shown with QCM-D. The main advantage of this grafting strategy is the use of aqueous system at room temperature.

Prior to all the characterization, modified nanofibers were thoroughly washed with water using centrifugation to remove all physically adsorbed peptide. ATR-FTIR analysis was performed to characterize and determine changes in the infrared bands related to the nisin immobilization on the CNF. Normalized FTIR spectra of the neat and grafted CNF are presented in Fig. 4. Unmodified CNF display several bands characteristics of cellulose at 3350 cm^{-1} (OH), 1110 cm^{-1} (C–O of secondary alcohol and used for the normalization of all spectra), and 2868 and 2970 cm^{-1} (C–H from $–CH_2–$).

In addition, TEMPO oxidized fibers also show a new peak 1550–1610 cm^{-1} corresponding to the asymmetric $–COO^-$ stretching from TEMPO CNF carboxylates. The spectra reported characteristic changes in the region of 1750–850 cm^{-1} due to the grafting of nisin on nanocellulose. The spectra of nisin-grafted CNF demonstrated distinct new characteristic bands at 1640 cm^{-1}, 1560 cm^{-1} and 1402 cm^{-1} associated with the presence of amide I group (C=O stretch combined with N–H deformation), amide II group (N–H deformation in amides combined with $–NH_3^+$ deformation), and amide III group (C–N stretch in primary amides combined with COO^- symmetric stretch in carboxylic acid salts), respectively.[50] The band around 2919 and 2849 has increased significantly after the addition or grafting of nisin. Moreover, direct mixing of the nisin into CNF demonstrated the band characteristic to both CNF and nisin.

Atomic force microscopy (Fig. 5) of unmodified CNF suspension showed the morphology of nanofibers in dimension of 18 ± 4 nm. Generally, the estimated diameter of TEMPO nanofibers should be around 3–4 nm 40. It is important to mention here that the mechanical treatment used in this investigation was ultra-friction grinding system, which provides nanofibers of higher dimension compared to nanofibers treated with homogenizer.[51] The average diameter of grafted CNF was 20 ± 7 nm and 21 ± 6 nm for CNF TEMPO-*g*-1eq. and CNF-TEMPO-*g*-4eq., respectively, which is not significantly different from unmodified CNF. In conclusion, no change in the morphology was observed after grafting owning to the non-

 This journal is © The Royal Society of Chemistry 2016

Published on 13 January 2016. Downloaded on 1/26/2026 10:23:08 AM.

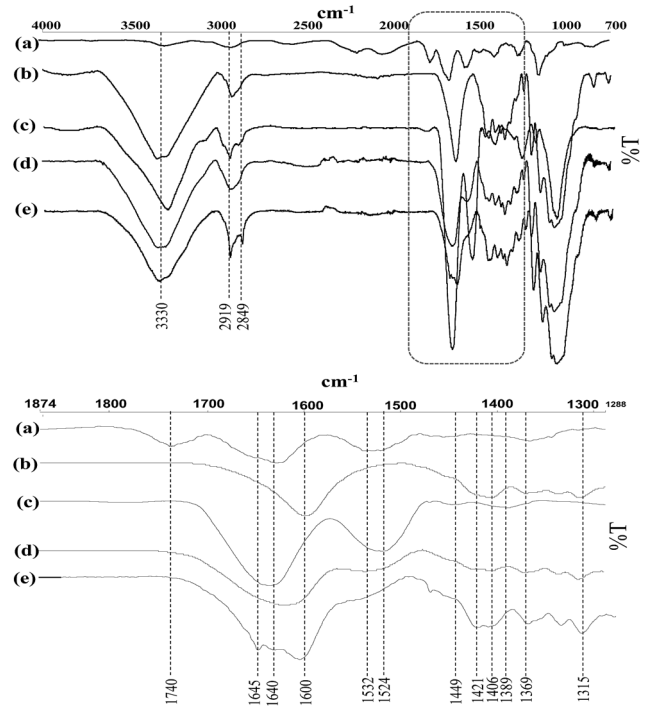

Fig. 4 FT-IR spectra of the (a) nisin, (b) CNF Tempo, (c) CNF Tempo-*m*-nisin (d) CNF Tempo-*g*-1-eq. and (e) CNF Tempo-*g*-4eq.

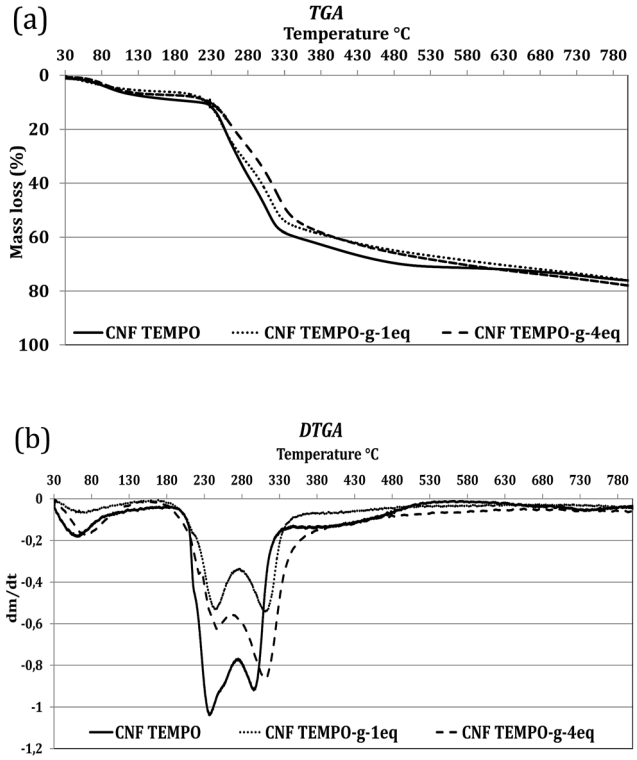

Fig. 6 Thermographs for the control (CNF and nisin) and grafted CNF with different initial concentrations.

swelling grafting solvent (MES buffer) used for the reaction process.

Apparent change in colour (from white to brown) was noticed after the grafting with the higher concentration of peptide of the film. In contrast, no change in colour was observed when the concentration used for grafting is 1 equivalent. This observation is in agreement with the FTIR results *i.e.* more pronounced bands were obtained with CNF Tempo-*g*-4eq.

Influence of peptide grafting on thermal degradation

Thermogravimetric analyses (TGA) were accomplished to determine the influence of nisin on the thermal stability of cellulose. Weight loss and derivative weight loss thermographs for reference and modified samples are represented in Fig. 6. The formation of sodium carboxylate groups from the C6 primary hydroxyls of cellulose microfibrils surfaces by the TEMPO oxidation affects the thermal degradation.

Degradation of TEMPO cellulose fibers starts at 200 °C under nitrogen while with the conventional cellulose, its decomposition start at 300 °C. The initial decreases in weight observed at about 60–100 °C in the reference TEMPO CNF is a consequence of the loss of the residual moisture. But, this depression in weight for residual moisture is slightly lower in the grafted samples stating the presence of less moisture comparatively after grafting which is classical for all grafting procedures.[52] As already shown in previous literature, small modification might prove undirectly the grafting. Indeed it is well-known that nanocellulose grafting with large molecule like

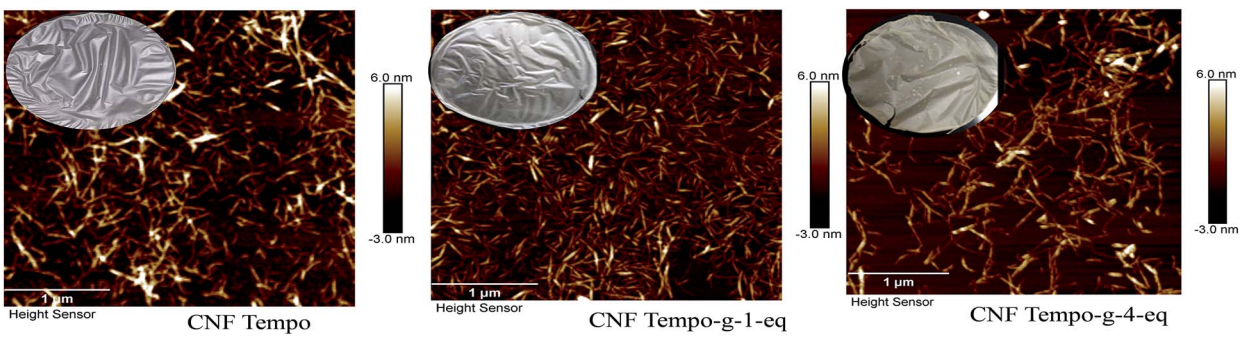

Fig. 5 AFM pictures of CNF Tempo, CNF Tempo-*g*-1-eq. and CNF Tempo-*g*-4eq. with films after grafting on the surface of cellulose (conc. 0.1%, tapping mode in air, area 3.3 × 3.3 μm^2).

Published on 13 January 2016. Downloaded on 1/26/2026 10:23:08 AM.

nisin can protect the nanocellulose from thermal degradation.[46,53,54]

As a result, grafting (or adsorption) of nisin on the CNF slightly improves the thermal stability of the cellulose (Table 1). 70% weight loss was obtained at 490 °C, 619 °C and 570 °C for CNF Tempo, CNF Tempo-*g*-1eq. and CNF Tempo-*g*-4eq., respectively. However, at higher temperatures, disintegration of nisin-grafted cellulose occurs, comparatively at lower temperature with the reference nanofibers due to the decomposition of grafting agent. Moreover, presence of higher quantity of nisin in CNF Tempo-*g*-4eq. makes it more sensitive to higher temperatures than the CNF Tempo-*g*-1eq.

The DTGA curves of TEMPO CNF demonstrate two evident peaks at 239 °C and 290 °C. The first peak in the DTGA curves come from the degradation of sodium anhydroglucuronate units, and the other peak at 290 °C indicates the thermally unstable anhydroglucuronate groups present at the crystal's surface. Grafting with nisin slightly enhances the stability of anhydroglucuronate groups present on the crystal surfaces. Thus, the second peak increases to the 309 °C and 305 °C for CNF Tempo-*g*-1eq. and CNF Tempo-*g*-4eq., respectively.

Quantification of peptide grafting on CNF

Nitrogen content for neat and grafted CNF are shown in Table 2 using bulk elemental analysis. With the grafting of nisin on CNF, there is high content of nitrogen in grafted CNF compared to the neat CNF which verifies the grafting of CNF. Moreover, when grafted with 4 equivalent of nisin, nitrogen content on grafted fibers increased to 2.9% compared to 1.8% of 1 equivalent CNF. Therefore, higher nitrogen content in grafted CNF is in accordance with the immobilization of nisin on the surface of nanocellulose.

The presence of carboxyl content on the surface of TEMPO CNF was used to calculate the grafting efficiency. Carboxyl content on the surface was analysed by conductomertic titration and found to be 1088, 787 and 590 mmol g^{-1} for CNF Tempo, CNF Tempo-*g*-1eq. and CNF Tempo-*g*-4eq. respectively. From these values, it was concluded that 27.5% of carboxyl group in CNF Tempo-*g*-1eq. and 45.7% in CNF Tempo-*g*-4eq. were modified with nisin.

Antibacterial activity of grafted CNF films

Qualitative assessment against *B. subtilis*. First, a qualitative test was done to check the antimicrobial activity of the non-grafted and grafted samples (Fig. 7). Neat CNF TEMPO was used as negative reference which did not demonstrate any activity against *B. subtilis*. Nisin mixed with CNF TEMPO was used as positive reference and an apparent zone of inhibition was formed around the sample after 3 days.[55]

Zone of inhibition was also formed by CNF Tempo-*g*-1-eq. and CNF Tempo-*g*-4eq. which can be attributed to the presence of non-covalent bonded nisin present in the CNF.

In a previous study, it was stated that uncontrolled and non-covalent immobilization of peptide forms an unstable layer but on the other hand activation of surface with EDC/NHS leads to the stable immobilization of peptide.[50] Furthermore, this hypothesis was also proved with Quartz crystal microbalance with dissipation (QCM-D).

Quantitative assessment against *B. subtilis* and *S. aureus*. In addition, the capability to grafted CNF was quantitatively analysed against two gram positive bacterial strains (*B. subtilis* and *S. aureus*) over 24 hours in contact. Again, CNF TEMPO and CNF TEMPO mixed with nisin (CNF Tempo-*m*-nisin) were used as negative and positive controls respectively. From the AFNOR qualitative test, it was evident that the antibacterial activity was by both active contact and leaching of nisin even after grafting. Therefore, first, the quantitative test was carried out with each sample without any further treatment.

It was observed that regardless of the concentration or method of nisin incorporation, complete killing effect was seen against *B. subtilis* (Fig. 7(ii)). After that, the authors tried to remove the non-immobilised or free nisin from inside the nanoporous structure of CNF by washing for 48 hours. Washing with water efficiently removes 94% (w/w) of the nisin which was recovered from CNF Tempo-*m*-nisin when the nisin physically mixed with CNF fibers, but from the grafted CNF, less than 1.6% (w/w) of the nisin was released.

Subsequently, antimicrobial activity was carried with these washed samples. Nevertheless, again complete killing was examined with *B. subtilis*. Despite, when treated with stronger and more resistant bacteria, *S. aureus*, physically mixed nisin after washing exhibited very low bactericidal activity but still showed a bacteriostatic activity with reduction of 0.7 log of the bacterial population over 24 hours. Moreover, this slight inhibition with CNF Tempo-*m*-nisin could be attributed to the nisin strongly crosslinked with CNF which is difficult to remove after washing.

Although, grafting with higher quantity (CNF Tempo-*g*-4eq.) illustrates a significant reduction of bacterial population after 24 hours *i.e.* 3.8 log CFU reduction. The different bacterial efficiency against *S. aureus* was obtained because of its high level of resistance abiding the effect of antimicrobials[56]_ENREF_53. Even more, grafted CNF at lower

Table 1 Temperature degradation profile at different relative weight loss for neat and nisin grafted CNF

Weight loss (%)	CNF Tempo	CNF Tempo-*g*-1eq.	CNF Tempo-*g*-4eq.
10	214	223	226
30	265	271	289
50	306	318	332
70	490	619	570
80	900	866	850

Table 2 Grafting efficiency of nisin on the surface of nanofibres

	Nitrogen content (%)	Carboxyl content (mmol g^{-1})	Grafting (%)
CNF Tempo	0	1087.5	
CNF Tempo-*g*-1eq.	1.8	787	27.5
CNF Tempo-*g*-4eq.	2.9	590	45.7

This journal is © The Royal Society of Chemistry 2016

Published on 13 January 2016. Downloaded on 1/26/2026 10:23:08 AM.

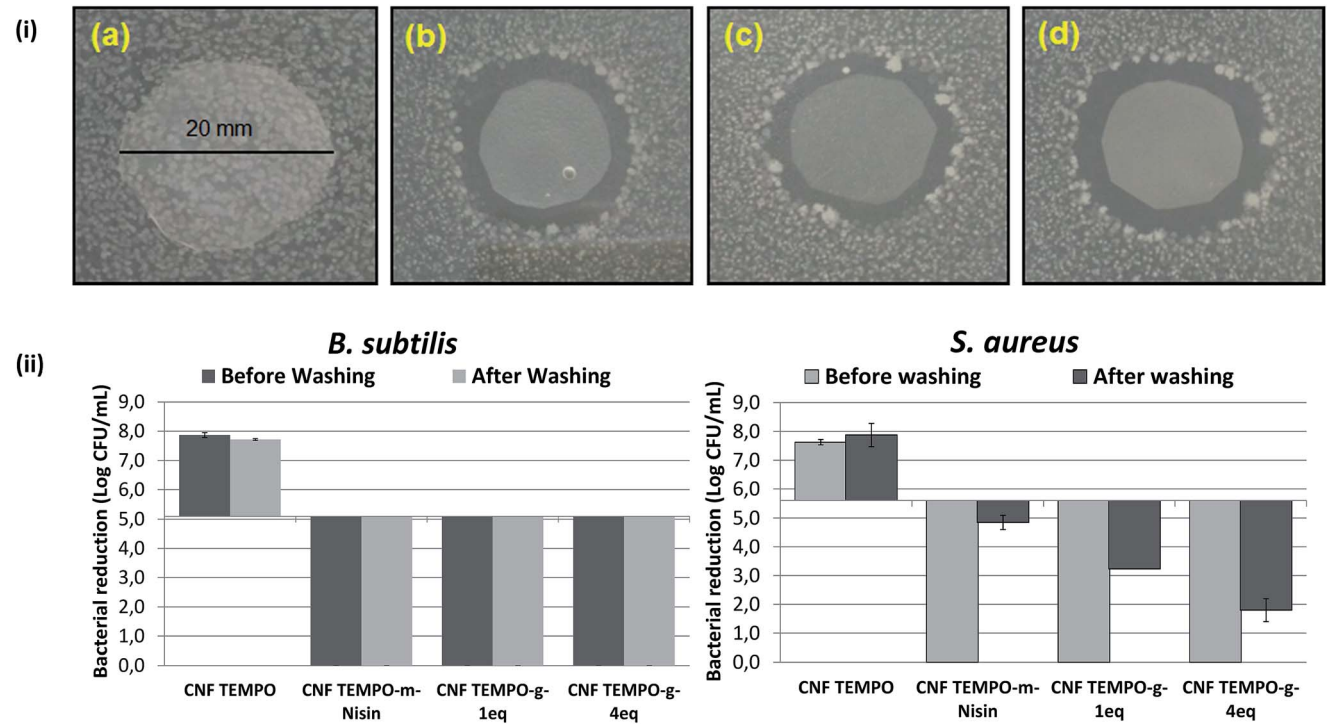

Fig. 7 (i) Qualitative analysis of grafting on antimicrobial activity of *B. subtilis*: (a) CNF Tempo (b) CNF Tempo-*m*-nisin (c) CNF Tempo-*g*-1-eq. (d) CNF Tempo-*g*-4eq., (ii) effect of nisin on antimicrobial activity of *Bacillus subtilis* and *Staphylococcus aureus* on CNF Tempo, CNF Tempo-*m*-nisin, CNF Tempo-*g*-1-eq., and CNF Tempo-*g*-4eq.

concentration (1 eq.) was successful, which is evident of bactericidal activity against these highly resistant bacteria.

Nisin classically used to preserve cheese or canned fruits and vegetable. These products retains significant amount of water which can wash off nisin from the packaging matrix. After grafting with nisin, peptide molecule stays on the surface of the matrix for longer period of time and provides longer shelf life to food products. In addition, the activity of nisin was not affected after grafting since only one amino group was changed among the large amount available.

Conclusions

In conclusion, nisin can be implemented with CNF either by direct incorporation or grafting on its surface. QCM-D confirmed the interface reaction between nisin and CNF with EDC/NHS but also gave evidence of the strong interaction between nisin and CNF without any coupling agent.

In this study, a two-step procedure was proposed and developed for fabrication of antimicrobial film. Surface modification of CNF was performed with an active molecule, nisin, was activated by using the coupling agents EDC/NHS. Surface functionalization was confirmed by the emergence of new band for amide group in FTIR and the presence of nitrogen after grafting. The presence of nisin improves thermal stability of CNF and washing of mixed nisin onto CNF is strongly more efficient than the grafted one.

Conversely, qualitative antimicrobial test against *B. subtilis* revealed the leaching of nisin from the grafted nanofibers film thanks to the strong interaction between the nisin and CNF. Direct mixing of nisin with CNF demonstrated complete killing against *B. subtilis* even after washing, but the activity decreases when applied to more resistant bacteria, *S. aureus*. Even after washing for 48 hours, high bacterial killing (2.4 log CNF Tempo-*g*-1-eq. and 3.8 log CNF Tempo-*g*-4eq.) was reported.

It is noteworthy that direct mixing loses its activity after the release of active molecule within the time period or in continuous washing by the liquid present in food formulation. The grafting ensures food preservation for a long period of time as molecules are situated at the surface of the packaging system.

Nevertheless, it can be inferred from all the characteristics that the peptide grafted CNF have outstanding potential in antimicrobial active food packaging for products like cheese or canned vegetables.

Acknowledgements

This research was supported by new generation packaging (NEWGENPAK) project of the seven framework program of European research under grant agreement no. 290098. LGP2 is part of the LabEx Tec 21 (Investissements d'Avenir – grant agreement no. ANR-11-LABX-0030) and of the Énergies du Futur and PolyNat Carnot Institutes (Investissements d'Avenir – grant agreements no. ANR-11-CARN-007-01 and ANR-11-CARN-030-01). This research was made possible thanks to the facilities of the TekLiCell platform funded by the Région Rhône-Alpes (ERDF: European regional development fund).

Published on 13 January 2016. Downloaded on 1/26/2026 10:23:08 AM.

References

1 *351,000 People Die of Food Poisoning Globally Every Year*, ed. A. Sifferlin, World Health Organisation, 2015, TIME.
2 P. Suppakul, J. Miltz, K. Sonneveld and S. W. Bigger, *J. Food Sci.*, 2003, **68**, 408–420.
3 L. Vermeiren, F. Devilghere, M. Ran beest, N. Kruijef and J. Debevere, *Trends Food Sci. Technol.*, 1999, **10**(3), 77–86.
4 A. Watthanaphanit, P. Supaphol, H. Tamura, S. Tokura and R. Rujiravanit, *Carbohydr. Polym.*, 2010, **79**, 738–746.
5 S. W. Ali, S. Rajendran and M. Joshi, *Carbohydr. Polym.*, 2011, **83**, 438–446.
6 D. S. Cha, J. H. Choi, M. S. Chinnan and H. J. Park, *Lebensm.-Wiss. Technol.*, 2002, **35**, 715–719.
7 D. Ding, F. Wang, X. Liu and C. Han, *Appl. Mech. Mater.*, 2015, **731**, 385–388.
8 R. D. Joerger, *Poult. Sci.*, 2003, **82**, 640–647.
9 European Food Safety Authority (EFSA), *The use of nisin (E 234) as a food additive*, EFSA, 2006, vol. 314, pp. 1–16.
10 J. Lubelski, R. Rink, R. Khusainov, G. N. Moll and O. P. Kuipers, *Cell. Mol. Life Sci.*, 2008, **65**, 455–476.
11 N. E. Kramer, H. E. Hasper, P. T. C. v. d. Bogaard, S. Morath, B. d. Kruijff, T. Hartung, E. J. Smid, E. Breukink, J. Kok and O. P. Kuipers, *Microbiology*, 2008, **154**, 1755–1762.
12 J. A. Auxier, K. F. Schilke and J. McGuire, *J. Food Prot.*, 2014, **6**, 1624–1629.
13 M. K. Heshmati, N. Hamdami, M. Shahedi, M. A. Hejazi, A. A. Motalebi and A. Nasirpour, *Food Sci. Technol. Res.*, 2013, **19**, 749–758.
14 A. Cagri, Z. Ustunol and E. T. Ryser, *J. Food Prot.*, 2004, **67**, 833–848.
15 S. Eswaranandam, N. Hettiarachchy and M. Johnson, *J. Food Sci.*, 2006, **69**, 79–84.
16 C. P. O. Resa, L. N. Gerschenson and R. J. Jagus, *Food Control*, 2014, **44**, 146–151.
17 A. La Storia, G. Mauriello, F. Villani and D. Ercolini, *Food Bioprocess Technol.*, 2013, **6**, 2770–2779.
18 M. E. Janes, S. Kooshesh and M. G. Johnson, *J. Food Sci.*, 2002, **67**, 2754–2757.
19 M. Guo, T. Z. Jin, L. Wang, O. J. Scullen and C. H. Sommers, *Food Control*, 2014, **40**, 64–70.
20 X. Qi, G. Poernomo, K. Wang, Y. Chen, M. B. Chan-Park, R. Xu and M. W. Chang, *Nanoscale*, 2011, **3**, 1874–1880.
21 J. Wan, J. B. Gordon, K. Muirhead, M. W. Hickey and M. J. Coventry, *Lett. Appl. Microbiol.*, 1997, **24**, 153–158.
22 K. Ku and B. S. Kyung, *J. Microbiol. Biotechnol.*, 2007, **17**, 520–523.
23 M. Millette, C. Le Tien, W. Smoragiewicz and M. Lacroix, *Food Control*, 2007, **18**, 878–884.
24 M. Imran, S. El-Fahmy, A. Revol-Junelles and S. Desobry, *Carbohydr. Polym.*, 2010, **81**, 219–225.
25 B. Matthews, S. Mangalasary, D. Darby and K. Cooksey, *Packag. Technol. Sci.*, 2010, **23**, 267–273.
26 A. F. Turbak, F. W. Snyder and K. R. Sandberg, *J. Appl. Polym. Sci.: Appl. Polym. Symp.*, 1983, **37**, 815–827.
27 K. Syverud and P. Stenius, *Cellulose*, 2009, **16**, 75–85.
28 I. Siro and D. Plackett, *Cellulose*, 2010, **17**, 459–494.
29 N. Lavoine, I. Desloges, A. Dufresne and J. Bras, *Carbohydr. Polym.*, 2012, **90**, 735–764.
30 K. L. Spence, R. A. Venditti, Y. Habibi, O. J. Rojas and J. J. Pawlak, *Bioresour. Technol.*, 2010, **101**, 5961–5968.
31 T. Saito, S. Kimura, Y. Nishiyama and A. Isogai, *Biomacromolecules*, 2007, **8**, 2485–2491.
32 Y. Habibi, *Chem. Soc. Rev.*, 2014, **43**, 1519–1542.
33 M. Andresen, P. Stenstad, T. Møretrø, S. Langsrud, K. Syverud, L. Johansson and P. Stenius, *Biomacromolecules*, 2007, **8**, 2149–2155.
34 S. Saini, M. N. Belgacem, J. Mendes, G. Elegir and J. Bras, *ACS Appl. Mater. Interfaces*, 2015, **7**, 18076–18085.
35 S. C. M. Fernandes, P. Sadocco, P. Teodoro, A. Alonso-Varona, A. Eceiza, A. J. D. Silvestre, I. Mondragon and C. S. R. Freire, *ACS Appl. Mater. Interfaces*, 2013, **5**, 3290–3297.
36 K. Missoum, P. Sadocco, J. Causio, M. N. Belgacem and J. Bras, *Mater. Sci. Eng., C*, 2014, **45**, 477–483.
37 S. Saini, M. N. Belgacem, K. Missoum and J. Bras, *Ind. Crops Prod.*, 2015, **78**, 82–90.
38 S. Saini, Ç. Yücel-Falco, M. N. Belgacem and B. Julien, *Carbohydr. Polym.*, 2016, **135**, 239–247.
39 S. Saini, M. N. Belgacem, M. C. Brochier Salon and J. Bras, *Cellulose*, 2016, **23**(1), 795–810.
40 A. Isogai, T. Saito and H. Fukuzumi, *Nanoscale*, 2011, **3**, 71–85.
41 G. Z. Sauerbrey, *Z. Phys.*, 1959, **155**, 206.
42 X. Turon, O. J. Rojas and R. S. Deinhammer, *Langmuir*, 2008, **24**, 3880–3887.
43 C. Aulin, E. Johansson, L. Wågberg and T. Lindstrom, *Biomacromolecules*, 2010, **11**, 872–882.
44 R. Bardet, V. Perrin, N. Belgacem and J. Bras, *ACS Appl. Mater. Interfaces*, 2015, **7**, 7.
45 H. Orelma, I. Filpponen, L.-S. Johansson, M. Osterberg, O. J. Rojas and J. Laine, *Biointerphases*, 2012, **7**, 61.
46 A. Benkaddour, K. Jradi, S. Robert and C. Daneault, *Nanomaterials*, 2013, **3**, 141–157.
47 I. Filpponen and D. S. Argyropoulos, *Biomacromolecules*, 2010, **11**, 1060–1066.
48 H. Orelma, I. Filpponen, L.-S. Johansson, M. Osterberg, O. J. Rojas and J. Laine, *Biointerphases*, 2012, **7**, 61.
49 H. Sadeghifar, I. Filpponen, S. P. Clarke, D. F. Brougham and D. S. Argyropoulos, *J. Mater. Sci.*, 2011, **46**, 7344–7355.
50 R. Mauchauffe, M. Moreno-Couranjou, N. D. Boscher, C. e. V. D. Weerdt, A.-S. Duwez and P. Choquet, *J. Mater. Chem. B*, 2014, **2**, 5168–5177.
51 O. Nechyporchuk, F. Pignon and N. Belgacem, *J. Mater. Sci.*, 2015, **50**, 531–541.
52 H. Fukuzumi, T. Saito, T. Iwata, Y. Kumamoto and A. Isogai, *Biomacromolecules*, 2009, **10**, 162–165.
53 K. Missoum, M. N. Belgacem and J. Bras, *Materials*, 2013, **6**, 1745–1766.
54 H. Lönnberg, L. Fogelström, S. Samir, L. A. Berglund, E. Malmström and A. Hult, *Eur. Polym. J.*, 2008, **44**, 2991–2997.
55 T. Huq, B. Riedl, J. Bouchard, S. Salmieri and M. Lacroix, *Cellulose*, 2014, **21**, 4309–4321.
56 I. T. Paulsen, T. G. Littlejohn, P. Rådström, L. Sundström, O. Sköld, G. Swedberg and R. A. Skurray, *Antimicrob. Agents Chemother.*, 1993, **37**, 761–768.

 This journal is © The Royal Society of Chemistry 2016